Coupling a DEM material model to multibody construction equipment

Michael Burger[1], Klaus Dreßler[1], Torbjörn Ekevid[2], Stefan Steidel[1], Dietmar Weber[1]

[1] Mathematical Methods in Dynamics and Durability
Fraunhofer Institute for Industrial Mathematics ITWM
Fraunhofer-Platz 1, 67663 Kaiserslautern, Germany
{michael.burger, klaus.dressler, stefan.steidel, dietmar.weber}@itwm.fraunhofer.de

[2] Virtual Product Development
Volvo Construction Equipment AB
Carl Lihnells väg, 360 42 Braås, Sweden
torbjorn.ekevid@volvo.com

Abstract

Particle simulation with the Discrete Element Method (DEM) is well-established and widely used in soil dynamics related applications. The wide range of applications can be envisaged, for instance, in automotive engineering, material handling and manufacturing. In recent years, the Fraunhofer ITWM has developed and implemented its own DEM code entitled »GRAnular Physics Engine (GRAPE)« which is currently specialized for granular materials. In this paper, we present the technical realization of GRAPE's communication interface in the construction equipment development context that has been evolved during a project collaboration between the Fraunhofer ITWM and Volvo CE. Moreover, we address numerical studies with a focus on GRAPE internal parameters and co-simulation settings by applying the interface to couple a multibody wheel loader model and a multibody hauler model, respectively.

Keywords: co-simulation, discrete element method, multibody dynamics, soil dynamics

1. Introduction

Particle simulation with the Discrete Element Method (DEM) is well-established and widely used in soil dynamics related applications. The wide range of applications can be envisaged, for instance, in automotive engineering (e.g. soil interaction with wheels or tracks, earth moving equipment, ...), material handling (e.g. conveyer belt load extraction, material spread in hopper, ...), manufacturing and processing (e.g. granulation or agglomeration of powders, crushing, grinding, ...). In this context, the Fraunhofer ITWM has developed and implemented its own DEM code entitled »GRAnular Physics Engine (GRAPE)« for modeling and simulating soft soil. In particular, we focus on the prediction of correct reaction forces – which implies the necessity of an appropriate model parameterization – and the capability in closed-loop scenarios, i.e. the particle interaction with external tools in a general sense.

Numerical system simulation plays an essential role in the modern product development process, since studying and evaluating product stages virtually and model-based can accelerate development cycles significantly. Given a tremendous usage variability in the area of construction machines, it is an important strategy to simulate different usage scenarios with appropriate numerical system models. To obtain reliable results in these simulations on, for instance, durability and performance properties of the respective machine, it is inevitable to model both, the machine itself and the interaction with the exterior environment, in a sufficient model quality. Thus, when considering construction equipment like excavators and wheel loaders, soil and the interaction with the machine during the digging process has to be modeled and simulated properly.

We exemplify the technical realization of GRAPE's application in the construction equipment development context that has been evolved during a bilateral project collaboration between the Fraunhofer ITWM and Volvo CE. In particular, we implement a co-simulation scenario that couples Volvo CE's multibody wheel loader model with GRAPE for soil simulation, in order to realize a framework in which different loading maneuvers can be simulated and analyzed. We conceptually establish a force-displacement coupling for the co-simulation setup, as illustrated in Figure 1, that is in principle not confined to the wheel loader model but can be straightforwardly transferred to a hauler or an excavator model, respectively.

The paper is structured as follows. In Section 2, we introduce some main facts and implementation details about GRAPE. Those are essential for the technical realization of the addressed coupling setup that is described in detail in Section 3. Moreover, we address applications and numerical studies of the developed coupling framework in Section 4. In particular, we present numerical studies with a focus on GRAPE internal parameters and co-simulation settings in case of the wheel loader coupling environment in Subsection 4.1, and illustrate the transferability of the setup by

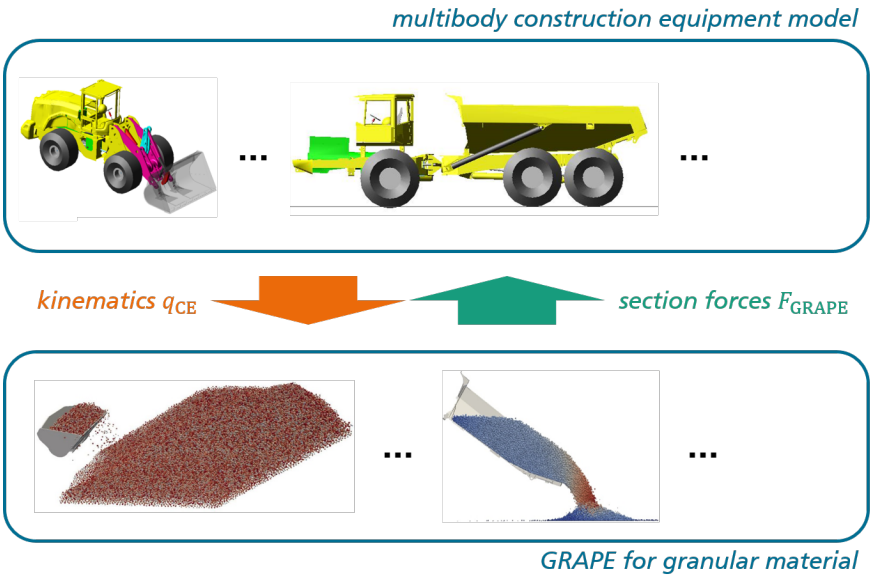

Figure 1: Principle concept for coupling GRAPE to multibody construction equipment

analyzing the tire forces of a hauler when discharging granular material in Subsection 4.2. Finally, we summarize the results and provide an outlook on further activities in Section 5.

2. Particle simulation

Particles within GRAPE are represented by 3-dimensional spheres with 3 translational degrees of freedom interacting with each other and external tools via contact forces. An external tool geometry is imported as a triangular mesh and internally treated as a rigid body. A major and time-consuming task consists in the *collision detection* between particles and particles with mesh triangles. Due to the complexity, the problem of collision detection is split into two phases of different timesteps – a *broad phase* and a *narrow phase* collision detection.

The *broad phase* collision detection only operates in every n^{th} timestep, for some natural number $n \in \mathbb{N}$. More precisely, the *broad phase* collision detection stepsize Δt_{bp} is an integer multiple of GRAPE's integration stepsize Δt_{GRAPE}, i.e. $\Delta t_{\text{bp}} = n \cdot \Delta t_{\text{GRAPE}}$. The *broad phase* performs a complete collision detection yielding a relatively small list of potential contacts for each particle. In particular, for a given particle the algorithm looks for neighbouring particles and external tools in a range defined by a fractional multiple τ of the maximal particle radius r_{max}, as illustrated in Figure 2.

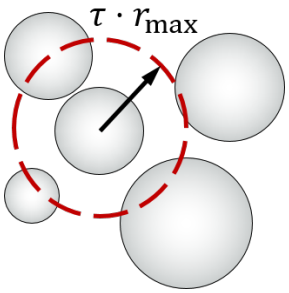

Figure 2: *Broad phase* collision detection

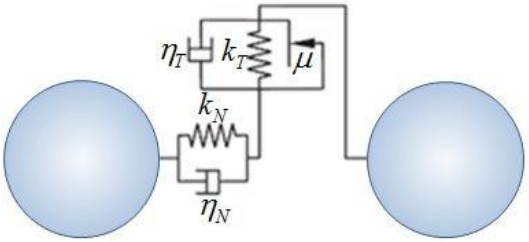

Figure 3: Schematic particle interaction

The *narrow phase* collision detection operates in every timestep, so that the *narrow phase* detection stepsize Δt_{np} is equal to GRAPE's integration stepsize Δt_{GRAPE}, i.e. $\Delta t_{\text{np}} = \Delta t_{\text{GRAPE}}$. The *narrow phase* collision detection checks the previously determined potential contact list for actual contacts by calculating the actual distance, and these respective contacts are considered for force interaction.

The implementation is strictly parallelized so that realtime factors well below 100 can be achieved for approximately 150000 particles and approximately 40000 triangles in the mesh. Moreover, GRAPE is operable in two basic modes – *standalone* and *interactive* for closed-loop scenarios. In the first case, GRAPE processes the instructions given by an input file and provides the requested results in a file-based system. In the second case, GRAPE operates in a server mode waiting for external requests. These requests are generally produced by an external application (e.g. an MBS program) through a GRAPE client which communicates with the GRAPE server.

More detailed information about GRAPE regarding the physical model and the model implementation are elaborated in [1, 2, 3, 4]. In a nutshell, the particles are geometrically represented by rigid spheres with disabled rotational degrees of freedom and the particle interaction force is in principle determined by five parameters – the normal stiffness k_N and damping η_N, the tangential stiffness k_T and damping η_T, and a friction coefficient μ – as qualitatively illustrated in Figure 3.

3. Coupling interface

In order to realize particle interaction with external tools in a general sense, we implement a generic interface to any multibody simulation tool that is aligned with the FMI 1.0 interface standard [5]. In this context, we interpret an external tool as a rigid body with its geometry represented and imported into GRAPE by a triangular mesh.

Within the project collaboration between the Fraunhofer ITWM and Volvo CE we explicitly develop a coupling framework between Volvo's multibody wheel loader model – modeled in MSC.Adams – and GRAPE for soil simulation, as already depicted in Figure 1. Consequently, we establish a force-displacement coupling for the co-simulation setup where the wheel loader bucket is modeled and simulated within GRAPE, the bucket section forces F_{GRAPE} (more precisely: forces F_{GRAPE} and torques M_{GRAPE}) are transmitted to the wheel loader model which, in turn, provides the bucket kinematic states q_{CE} (more precisely: displacements q_{CE} and Euler angles α_{CE}) for GRAPE. To sum up, we obtain the following situation:

$$\dot{x}_{\text{CE}} = f_{\text{CE}}\left(x_{\text{CE}}, u_{\text{CE}} = F_{\text{GRAPE}}\right) \tag{1}$$

$$q_{\text{CE}} = g_{\text{CE}}\left(x_{\text{CE}}\right) \tag{2}$$

$$\dot{x}_{\text{GRAPE}} = f_{\text{GRAPE}}\left(x_{\text{GRAPE}}, u_{\text{GRAPE}} = q_{\text{CE}}\right) \tag{3}$$

$$F_{\text{GRAPE}} = g_{\text{GRAPE}}\left(x_{\text{GRAPE}}\right) \tag{4}$$

with states x_{CE}, inputs u_{CE} for the construction equipment model and states x_{GRAPE}, inputs u_{GRAPE} for GRAPE. The exchange of the coupling quantities $u_{\text{CE}} = F_{\text{GRAPE}}$ and $u_{\text{GRAPE}} = q_{\text{CE}}$ is organized in a parallel scheme for efficient co-simulation, as illustrated in Figure 4. *Subsystem 1* (the multibody construction equipment model) provides kinematic states $q_i = q_{\text{CE}}$ as input for *Subsystem 2* (GRAPE) which, vice versa, provides section forces $F_i = F_{\text{GRAPE}}$ as input for *Subsystem 1*. The data exchange takes place at each macro time point t_i together with data-based prediction $q^{pred} = \pi_q(q_i, q_{i-1}, \ldots)$ for the kinematic states and $F^{pred} = \pi_F(F_i, F_{i-1}, \ldots)$ for the section forces, respectively. In the subsequent macro time step $t_i \rightarrow t_{i+1}$ both subsystems operate with the predicted coupling quantities $u_{\text{CE}}(t) = F^{pred}(t)$ and $u_{\text{GRAPE}}(t) = q^{pred}(t)$.

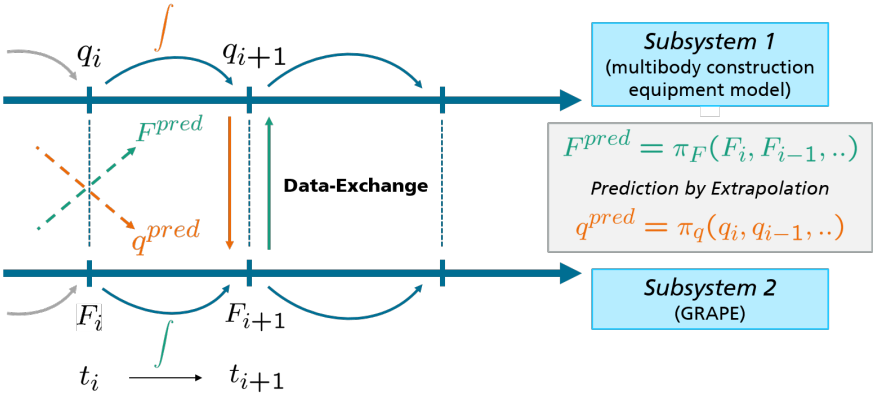

Figure 4: Parallel co-simulation scheme for coupling GRAPE to multibody construction equipment

The realization of the prescribed coupling concept requires specific co-simulation interfaces for the multibody construction equipment model and the GRAPE particles, as well as a co-simulation master algorithm organizing the data

exchange and the prediction strategies. In this connection, MATLAB/Simulink is chosen as the platform for setting up the co-simulation scenario. One the one hand, we utilize the plant export to MATLAB provided by MSC.Adams (*Adams Plant*) and, on the other hand, GRAPE is integrated as an S-Function into the scheme (*DEM S-Function*). Additionally, the co-simulation master is implemented in a MATLAB/Simulink subsystem (*Co-Simulation Master*). The communication, i.e. the exchange of the coupling quantities, with the GRAPE server is realized via a TCP/IP network protocol so that it is possible to run GRAPE and MATLAB/Simulink together with MSC.Adams on different host PC's, as depicted in Figure 5.

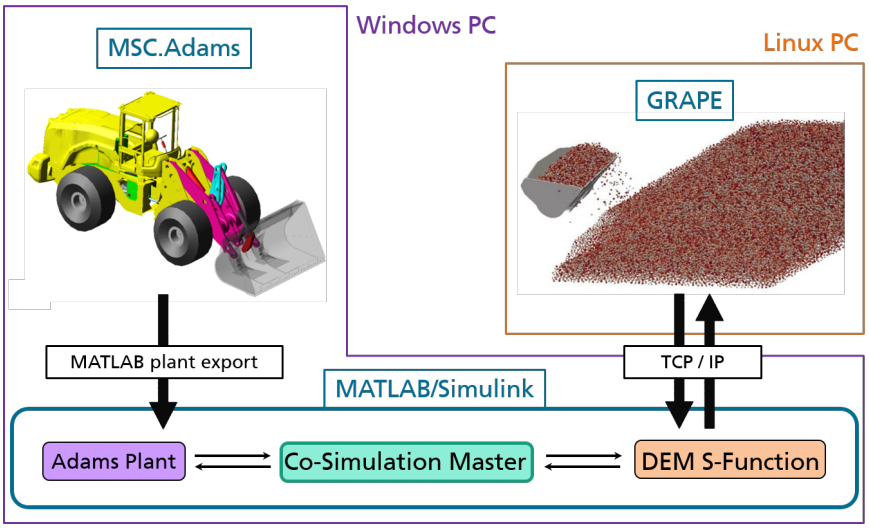

Figure 5: Realization of co-simulation scenario for coupling GRAPE to multibody construction equipment

The presented coupling interface is not confined to the multibody wheel loader model as investigated in the mentioned bilateral project, but can easily be adapted to further multibody construction equipment models, see Section 4.

4. Applications and numerical studies

In this section, the prescribed co-simulation environment is adjusted, on the one hand, to couple GRAPE with Volvo's multibody wheel loader model for predicting bucket section forces during loading maneuvers in Subsection 4.1 and, on the other hand, to couple GRAPE with Volvo's hauler model for predicting wheel forces during discharge maneuvers in Subsection 4.2.

4.1. Wheel loader coupling

A validation of the wheel loader coupling environment by comparing simulation results with existing real measurements is properly presented in [6]. In this subsection, we moreover address the sensitivity of the setup by means of numerical studies with a focus on GRAPE internal parameters and co-simulation settings. We particularly vary the macro stepsize Δt_{macro}, as well as the particle normal stiffness k_N by independent studies. In this connection, we examine the section forces in the **A**- and **J**-bearing, respectively, where the bucket is connected to the lifting framework, as depicted in Figure 6. The section forces are represented in the bucket coordinate system.

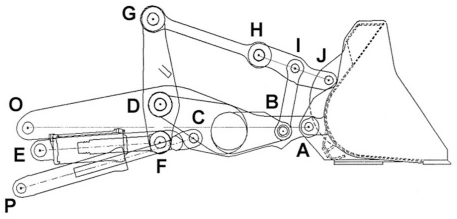

Figure 6: Bearing notations in the wheel loader lifting framework

The corresponding simulations are particularly prescribing the bucket filling phase, i.e. the first 15 seconds, of a certain loading maneuver. The data-based prediction strategy is always chosen *linear* regarding the kinematic states q^{pred} and

constant regarding the section forces F^{pred}:

$$q^{pred}(t) = \pi_q(q_i, q_{i-1}, t) = q_{i-1} + \frac{q_i - q_{i-1}}{\Delta t_{\text{macro}}} \cdot (t - t_{i-1}), \quad \text{for } t \in [t_i, t_{i+1}] \tag{5}$$

$$F^{pred}(t) = \pi_F(F_i, t) = F_i, \quad \text{for } t \in [t_i, t_{i+1}] \tag{6}$$

The following two paragraphs describe both respective parameter studies in more detail.

4.1.1. Macro stepsize

Within this parameter study, we vary the communication or macro stepsize according to

$$\Delta t_{\text{macro}} \in \{2 \cdot 10^{-3} s, 1 \cdot 10^{-3} s, 5 \cdot 10^{-4} s\} \tag{7}$$

where, at the same time, we keep the following parameters constant: GRAPE's integration stepsize $\Delta t_{\text{GRAPE}} = 10^{-4} s$, the *broad phase* detection stepsize $\Delta t_{\text{bp}} = 5 \cdot \Delta t_{\text{GRAPE}} = 5 \cdot 10^{-4} s$ and the particle normal stiffness $k_N = 4 \cdot 10^7$ Pa. The corresponding simulation results are depicted in Figure 7.

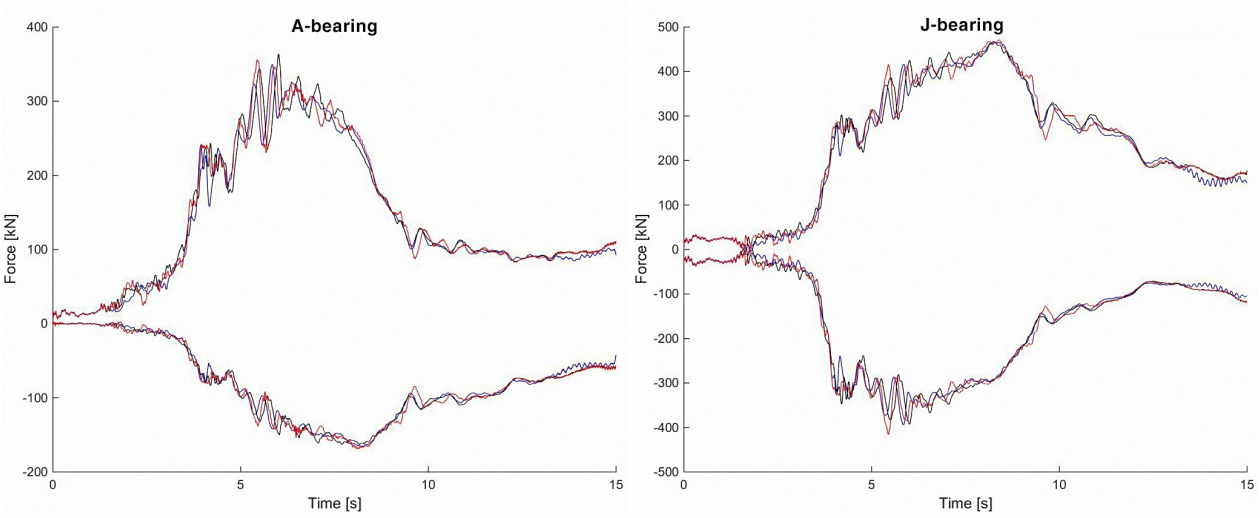

Figure 7: Longitudinal and vertical section forces in the **A**-bearing (left) and **J**-bearing (right) represented in the bucket frame obtained from parameter study by varying the macro stepsize $\Delta t_{\text{macro}} \in \{2 \cdot 10^{-3} s$ (blue), $1 \cdot 10^{-3} s$ (black), $5 \cdot 10^{-4} s$ (red)$\}$

At first sight, the communication stepsize does not significantly effect the considered section forces in this parameter range. This suggests that the prediction strategy is sufficiently accurate and robust, at least for relatively smooth loading maneuvers. This observation has to be investigated in more detail by considering loading trajectories of higher dynamics in combination with higher order extrapolation.

4.1.2. Particle normal stiffness

Within this parameter study, we vary the particle normal stiffness according to

$$k_N \in \{4 \cdot 10^7 \,\text{Pa}, 4 \cdot 10^8 \,\text{Pa}, 4 \cdot 10^5 \,\text{Pa}\} \tag{8}$$

where, at the same time, we keep the following parameters constant: GRAPE's integration stepsize $\Delta t_{\text{GRAPE}} = 10^{-4} s$, the *broad phase* detection stepsize $\Delta t_{\text{bp}} = 2 \cdot \Delta t_{\text{GRAPE}} = 2 \cdot 10^{-4} s$ and the communication or macro stepsize $\Delta t_{\text{macro}} = 4 \cdot 10^{-4} s$. The corresponding simulation results are depicted in Figure 8.

Given the large parameter variations over three orders of magnitude the force variations are comparatively moderate. We notice small deviations between $k_N = 4 \cdot 10^8$ Pa and $k_N = 4 \cdot 10^7$ Pa, but appreciable deviations between $k_N = 4 \cdot 10^7$ Pa and $k_N = 4 \cdot 10^5$ Pa. This observation may again be caused by the special cutting type of maneuver where

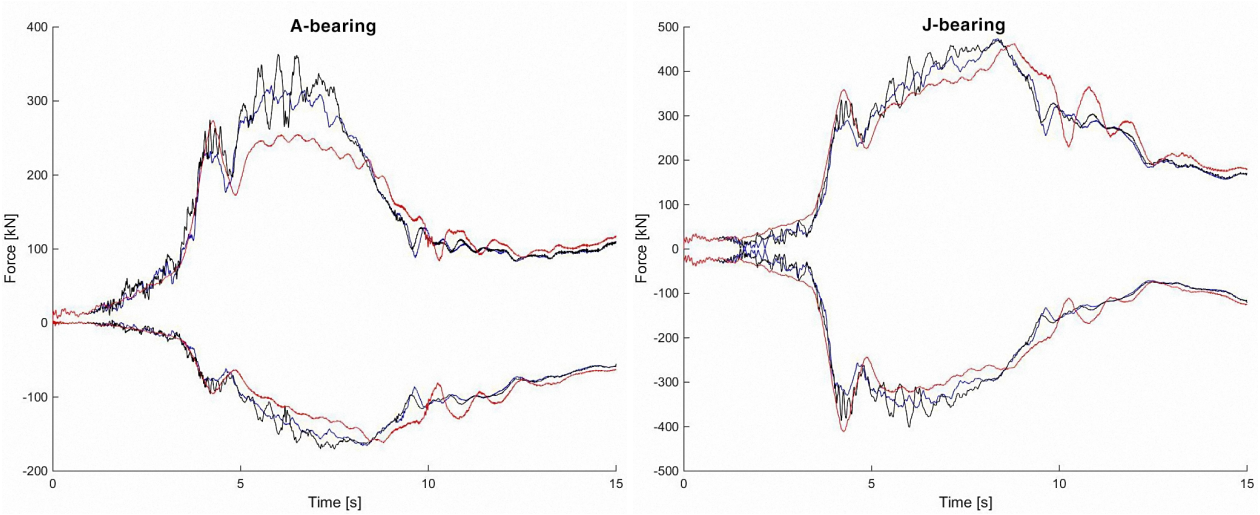

Figure 8: Longitudinal and vertical section forces in the **A**-bearing (left) and **J**-bearing (right) represented in the bucket frame obtained from parameter study by varying the particle normal stiffness $k_N \in \{4 \cdot 10^7\,\text{Pa}$ (blue), $4 \cdot 10^8\,\text{Pa}$ (black), $4 \cdot 10^5\,\text{Pa}$ (red)$\}$

no boundary constraints effect the particle movement in normal direction. Different experiments, particularly GRAPE parameterization experiments (triaxial tests), reveal a stronger influence of the particle normal stiffness k_N on the section forces. Since k_N usually represents the spring of highest stiffness, i.e. $k_N > k_T$, that dominates GRAPE's maximal integration stepsize via $\Delta t_{\text{GRAPE}} \sim k_N^{-1/2}$, the prescribed parameter study can serve to optimize the overall simulation time. To sum up, the normal stiffness parameter influences the numerical stability where stiff material can lead to a smaller integration stepsize. In further investigations, we will also study the tangential parameters k_T and μ as these might have a stronger sensitivity.

4.2. Hauler coupling

The coupling interface which is introduced in Section 3 is originally applied in a wheel loader environment. Anyway, due to its generality, it can be transferred to further multibody construction equipment. In this Subsection we exemplarily describe the adaption to a multibody hauler model in order to predict the occuring tire forces when discharging soil from the hauler's body, as illustrated in Figure 9.

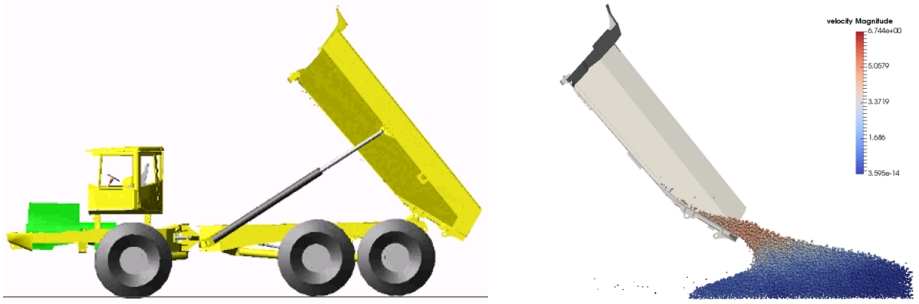

Figure 9: Screenshot of discharging the hauler

The hauler model has one *front axle* and two *rear axles*. We focus on the longitudinal and vertical tire forces at each axle. The simulation results, in particular the longitudinal and vertical tire forces obtained at the *front axle* during discharging are shown in Figure 10. The respective longitudinal and vertical tire forces obtained at both *rear axles* are shown in Figure 11. All tire forces are given in the TYDEX (TYre Data EXchange) C-axis system (center axis system), cf. [7].

We observe non-zero longitudinal forces at all axles ($t \in [8s, 12s]$) because of the material flow. All axes are equipped with hydraulic suspension elements. During the unloading phase, the accumulators fill the suspension elements due

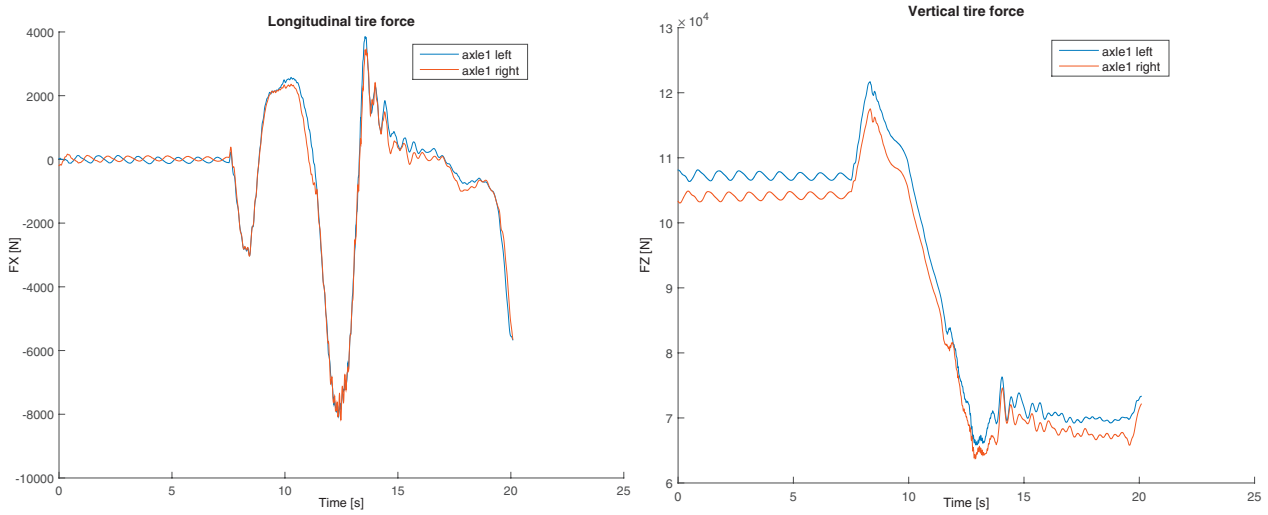

Figure 10: Longitudinal (left) and vertical (right) tire forces at the hauler's *front axle* represented in the TYDEX C-coordinate system during discharging the hauler's body

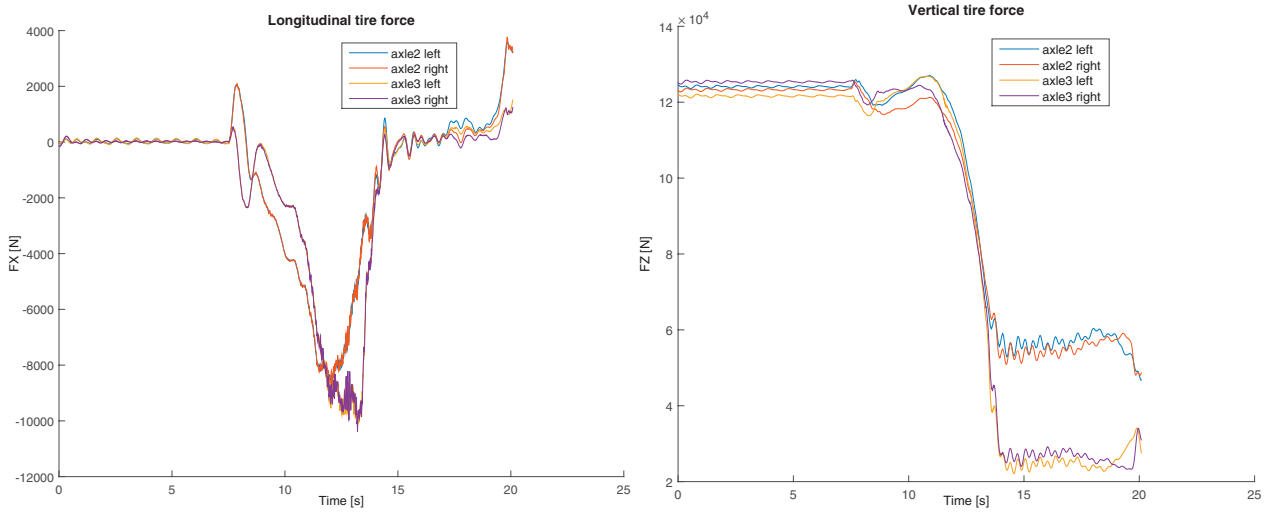

Figure 11: Longitudinal (left) and vertical (right) tire forces at the hauler's *rear axles* represented in the TYDEX C-coordinate system during discharging the hauler's body

to the decreased vertical forces. This means that the hauler will also rise in the rear during unloading after first being compressed due to the changed weight distribution. After discharging, the suspension elements have reached their maximum length – resulting in an uneven vertical force distribution between the 2nd and 3rd axle – before the control system starts to drain the cylinders with the aim to reach the target ride-height again. During the timespan when the cylinders retain their maximum length ($t \in [14s, 19s]$), the hydraulic bogie does not work as an actual hydraulic bogie that distributes the forces equally. Thereafter, the hauler will reach its target ride-height again, but the simulation is interrupted before this happens. Considering the front axle forces, sticky material or material with high internal friction may even cause the front axle to almost lose its contact to the ground while discharging if the machine layout is not set up properly.

5. Conclusion

In this article, we present a coupling framework of the »GRAnular Physics Engine (GRAPE)« to multibody construction equipment models. In particular, we address the schematic as well as the technical realization and illustrate its functionality by realizing a co-simulation setup to both a multibody wheel loader and a multibody hauler model. The numerical parameter studies reveal that the setup is robust and sufficiently accurate as to variations of the communication stepsize and the particle normal stiffness, at least for the considered loading maneuver. The picture may change for

different loading maneuvers of higher dynamics and significant modifications of the soil material parameters. Therefore, we especially have to investigate in studying the variation of the particle tangential stiffness and friction coefficient. Anyway, the simulation results are of good quality and can particularly be aligned with real experiments.

References

[1] M. Obermayr, K. Dreßler, C. Vrettos, P. Eberhard. A bonded-particle model for cemented sand. Computers and Geotechnics, 49:299-313, 2013.

[2] M. Obermayr. Prediction of Load Data for Construction Equipment using the Discrete Element Method. PhD thesis, University of Stuttgart, 2013.

[3] M. Obermayr, C. Vrettos, P. Eberhard, T. Däuwel. A discrete element model and its experimental validation for the prediction of draft forces in cohesive soil. Journal of Terramechanics, 53:93-104, 2014.

[4] J. Kleinert, B. Simeon, M. Obermayr. An inexact interior point method for the large-scale simulation of granular material. Computer Methods in Applied Mechanics and Engineering, 278:567-598, 2014.

[5] Modelica Association Project. Functional Mock-up Interface (FMI). https://www.fmi-standard.org.

[6] M. Balzer, M. Burger, T. Däuwel, T. Ekevid, S. Steidel, D. Weber. Coupling DEM Particles to MBS Wheel Loader via Co-Simulation. In K. Berns et. al., editors, Proceedings of the 4th Commercial Vehicle Technology Symposium (CVT 2016), pages 479-488. University of Kaiserslautern, 2016.

[7] H.-J. Unrau, J. Zamow. TYDEX-Format, Description and Reference Manual, Release 1.3. Initiated by the TYDEX Workshop, 1996.

[8] F. Henriksson, J. Minta. Bucket-soil interaction for wheel loaders – An application of the Discrete Element Method. Master thesis, Linnaeus University, 2016.